



## A Comparison of Dry Plasma and Wet Chemical Etching of GaSb Photodiodes

Vinay Bhagwat,<sup>a</sup> J. P. Langer,<sup>a</sup> Ishwara Bhat,<sup>a</sup> P. S. Dutta,<sup>a,z</sup> Tamer Refaat,<sup>b</sup> and M. Nurul Abedin<sup>c</sup>

<sup>a</sup>Center for Integrated Electronics, Rensselaer Polytechnic Institute, Troy, New York 12180, USA

<sup>b</sup>Science and Technology Corporation and <sup>c</sup>NASA Langley Research Center, Hampton, Virginia 23681-2199, USA

We report on the performance of GaSb pn junction photodiodes fabricated using electron cyclotron resonance plasma etching using  $\text{Cl}_2/\text{Ar}$  recipe, a mixed gas recipe consisting of  $\text{Cl}_2/\text{BCl}_3/\text{CH}_4/\text{Ar}/\text{H}_2$  and wet chemical etching. Diodes fabricated using  $\text{Cl}_2/\text{BCl}_3/\text{CH}_4/\text{Ar}/\text{H}_2$  recipe show an order of magnitude lower leakage current density and lower ideality factor. The highest value of the zero bias dynamic resistance-area product was obtained for  $\text{Cl}_2/\text{BCl}_3/\text{CH}_4/\text{Ar}/\text{H}_2$  etched diodes and was equal to  $830 \Omega \text{ cm}^2$  as compared to  $300 \Omega \text{ cm}^2$  for  $\text{Cl}_2/\text{Ar}$  and  $330 \Omega \text{ cm}^2$  for wet etching. Spectral responsivity of  $\text{Cl}_2/\text{BCl}_3/\text{CH}_4/\text{Ar}/\text{H}_2$  etched diodes was observed to be three times that of  $\text{Cl}_2/\text{Ar}$  and wet etched diodes. Overall, the diodes etched using the recently reported  $\text{Cl}_2/\text{BCl}_3/\text{CH}_4/\text{Ar}/\text{H}_2$  recipe provided the best optical and electrical characteristics.  
© 2004 The Electrochemical Society. [DOI: 10.1149/1.1691551] All rights reserved.

Manuscript submitted October 3, 2003; revised manuscript received November 25, 2003. Available electronically April 12, 2004

Recently, there is increasing interest in the gallium antimonide (GaSb) based compound semiconductors due to its wide range of optoelectronic applications in the mid-infrared (MIR) wavelengths.<sup>1</sup> GaSb is an attractive choice as a substrate material because its lattice parameter matches various ternary and quaternary III-V compound semiconductors whose band gaps cover a wide spectral range from  $\sim 0.3$  to  $1.58 \text{ eV}$ , *i.e.*,  $0.8\text{--}4.3 \mu\text{m}$ . High quantum efficiency photodetectors,<sup>2,3</sup> photovoltaic cells,<sup>4,5</sup> and laser diodes with low threshold current<sup>6,7</sup> have been demonstrated using GaSb and related compounds. Fabrication of these devices requires etching to form mesa or line structures. Despite the damage associated with dry etching, it can provide highly anisotropic profiles with good reproducibility and uniformity, and therefore is desirable compared to wet chemical etching. In spite of the technological importance of GaSb based alloys, little has been reported on the dry etching of GaSb and related materials.

A common choice of plasma chemistries for dry etching of GaSb-based structures consists of chlorine based precursors, such as  $\text{SiCl}_4$ ,  $\text{BCl}_3$ , or  $\text{Cl}_2$  because the volatilities of the gallium and antimony chlorides are generally very high.<sup>8</sup> Also, high-density plasma sources, such as electron cyclotron resonance (ECR), are preferred because of the increased density of low energy ions in the plasma.<sup>9</sup> Pearton *et al.*<sup>10,11</sup> have reported on the etching of GaSb in high density plasma using  $\text{Cl}_2/\text{Ar}$  and  $\text{BCl}_3/\text{Ar}$  chemistries down to  $-30^\circ\text{C}$ . Improvement in the anisotropy was observed at lower temperatures but at the cost of a decrease in the etch rates. They also observed that the surface morphology obtained by  $\text{BCl}_3/\text{Ar}$  etching was smoother than that of  $\text{Cl}_2/\text{Ar}$ .<sup>10</sup> Dry etching of GaSb using methane/hydrogen ( $\text{CH}_4/\text{H}_2$ ) and ethane/hydrogen ( $\text{C}_2\text{H}_6/\text{H}_2$ ) chemistry has also been reported.<sup>12,13</sup>  $\text{C}_2\text{H}_6$ -based plasmas show 50% higher etching rates as compared to the  $\text{CH}_4$ -based plasmas.<sup>13</sup> Addition of a polymer forming gas such as  $\text{CH}_4$  results in the formation of a polymeric thin film on the sidewalls, which minimizes the undercutting and provides passivation.<sup>14,15</sup> Although mixed chlorine and methane etches have been reported for various III-V compound semiconductors, systematic studies of antimonide are very few.<sup>16</sup> Langer *et al.* have recently reported a mixed-gas etching recipe consisting of chlorine, boron trichloride, methane, hydrogen, and argon ( $\text{Cl}_2/\text{BCl}_3/\text{CH}_4/\text{Ar}/\text{H}_2$ ) which shows high etching rate of  $0.5 \mu\text{m}/\text{min}$  and results into smooth surfaces and sharp sidewalls at room temperature.<sup>17</sup>

The effect of etching conditions on the device performance of GaSb and related materials has not been well addressed in the lit-

erature. In this paper, we have compared the performance of pn junction photodiodes fabricated using a  $\text{Cl}_2/\text{Ar}$  recipe roughly based on the results reported by Pearton *et al.*<sup>10,18</sup> a mixed gas recipe consisting of  $\text{Cl}_2/\text{BCl}_3/\text{CH}_4/\text{Ar}/\text{H}_2$ ,<sup>17</sup> and wet chemical etching using a NaK tartrate based recipe.

### Experimental

The substrates used in this study were (100) n-type GaSb (Te doped) obtained from Galaxy Compound Semiconductor Inc. The carrier concentration was  $5 \times 10^{17} \text{ cm}^{-3}$ . The substrates were degreased with hot xylene followed by acetone and methanol rinse (XAM cleaning). Then the samples were etched in hydrochloric acid (HCl) to remove the native oxide layer. Zinc (Zn) acts as p-type impurity in GaSb. Zn diffusion was carried out at  $500^\circ\text{C}$  for 5 h using the leaky box technique.<sup>19</sup> Solid Zn pellets were used as the source. The samples were next subjected to backside etching using a 2% solution of bromine in methanol for 30 s. Back side contacts were formed by electron beam (E-beam) evaporation of  $200 \text{ \AA}$  of tin and  $1000 \text{ \AA}$  of gold; followed by rapid thermal annealing (RTA) at  $350^\circ\text{C}$  for 5 s.

The front side metal contact consisted of  $400 \text{ \AA}$  titanium followed by  $800 \text{ \AA}$  gold evaporated using E-beam. The final step in the fabrication process was the mesa etching. The front metal contacts were protected using a photoresist and the mesa areas were patterned. The photoresist was cured by baking at  $110^\circ\text{C}$  for 10 min. A Plasmatherm Electron Cyclotron Resonance 357 system with a load-locked chamber was used for the dry etching of GaSb. One sample set was etched using  $\text{Cl}_2/\text{Ar}$  plasma. The gases were in the ratio of 1:6 at a pressure of 1.5 mTorr. 100 W rf power and 300 W plasma power was used and the temperature was maintained at  $-30^\circ\text{C}$ . The etch rate obtained with this process was  $135 \text{ nm}/\text{min}$ . A  $\text{Cl}_2/\text{BCl}_3/\text{CH}_4/\text{Ar}/\text{H}_2$  gas mixture in the ratio 2:1:2:6:12 was used to etch the second set of samples. A chamber pressure of 1.3 mTorr, rf power of 150 W, and plasma power of 400 W was used. The etching was carried out at room temperature. This recipe gave an etch rate of about  $560 \text{ nm}/\text{min}$ . The details of the surface morphology after etching are presented elsewhere.<sup>17</sup> The third sample set was prepared by wet etching. For the wet etching of GaSb, a mixture of  $\text{HCl}:\text{H}_2\text{O}_2:\text{NaK tartrate}$  (66 ml:18 ml:24 g in 1 liter of solution) was used. The etching rate with this solution was  $120 \text{ nm}/\text{min}$ . After the dry/wet-etching step, the photoresist was removed by using acetone and the samples were cleaned by XAM cleaning. Thereafter, the samples were rinsed in pure methanol to avoid the formation of oxide on the sidewalls, which increases the leakage current associated with the diodes. No surface passivation was carried out and no

<sup>z</sup> Email: duttap@rpi.edu

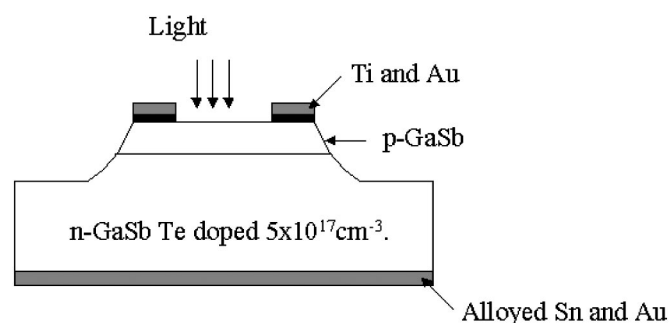


Figure 1. Schematic showing the cross-section of the device structure.

antireflective coating was applied. The schematic of the device structure is shown in Fig. 1.

### Results and Discussion

Because all of the devices had gone through the same processing except for the final mesa-etching step, the disparity in the performance of the diodes can be easily attributed to the different etching conditions. In this section, the current density-voltage (J-V), the zero bias dynamic resistance-area product ( $R_0A$ ) and the spectral responsivity characteristics of these diodes are discussed.

**Current-voltage (I-V) characteristics.**—I-V measurements under dark conditions were carried out using HP4140B I-V meter. Standard pin probes were used to make contact to the device. The measurements were carried out under ambient temperature and humidity. The electrical properties of the diodes as measured from time to time did not show any change. Figure 2 shows the J-V characteristics for the GaSb photodiodes etched using  $\text{Cl}_2/\text{Ar}$ ,  $\text{Cl}_2/\text{BCl}_3/\text{CH}_4/\text{Ar}/\text{H}_2$  gas mixture and wet chemical etching, under dark conditions at room temperature. This plot is representative of all the diodes tested on these samples with sizes varying from 100  $\mu\text{m}$  to 1 mm. The absolute value of the current density is plotted on a log scale as a function of applied voltage. The reverse bias leakage current density for  $\text{Cl}_2/\text{BCl}_3/\text{CH}_4/\text{Ar}/\text{H}_2$  etched diodes is an order of magnitude lower than that of  $\text{Cl}_2/\text{Ar}$  and wet etched diodes. Samples etched with the NaK tartrate based solution and the  $\text{Cl}_2/\text{Ar}$  plasma show very similar leakage characteristics. This indicates that by optimizing conditions for dry etching and using high-density plasma, devices showing same or even better performance as compared to wet etched diodes can be fabricated. The saturation

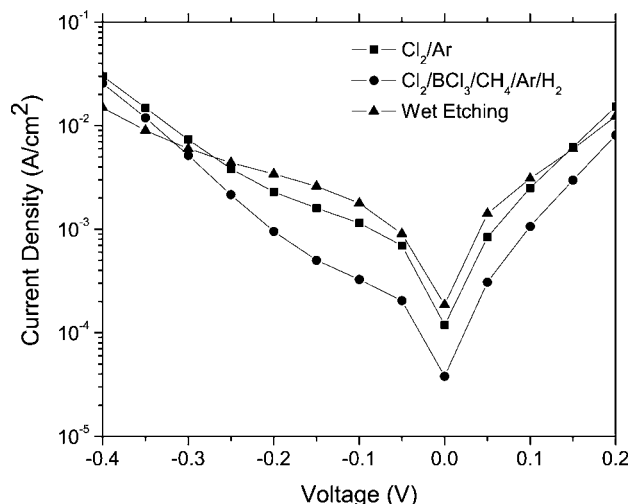


Figure 2. Current density-voltage (J-V) characteristics at room temperature and under dark conditions.

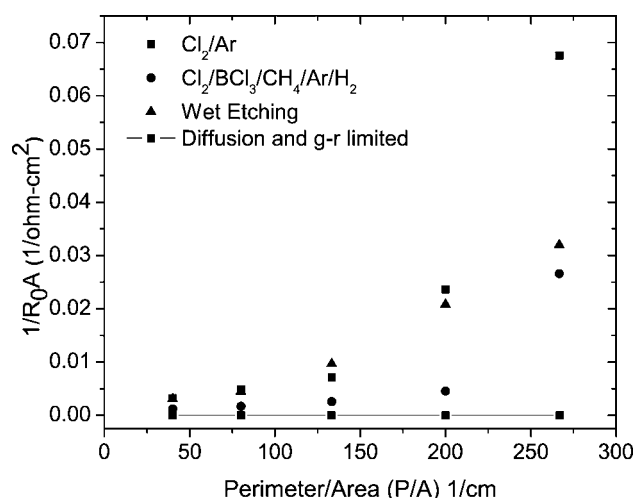


Figure 3. Inverse of the zero bias dynamic resistance-area product as a function of perimeter to area ratio for diodes etched using different chemistries.

current densities extracted from the I-V characteristics were  $4 \times 10^{-4}$ ,  $8 \times 10^{-5}$ , and  $6 \times 10^{-4}$   $\text{A}/\text{cm}^2$  for  $\text{Cl}_2/\text{Ar}$ ,  $\text{Cl}_2/\text{BCl}_3/\text{CH}_4/\text{Ar}/\text{H}_2$ , and wet etched diodes, respectively. The ideality factor for  $\text{Cl}_2/\text{BCl}_3/\text{CH}_4/\text{Ar}/\text{H}_2$  etched diodes was 1.87 as opposed to 2.1 for  $\text{Cl}_2/\text{Ar}$  and wet etched diodes. Use of the mixed chlorine and methane chemistry shows an improvement over both the wet etching and the previously reported chlorine mixture.

Figure 3 shows the inverse of the zero bias dynamic resistance-area product ( $1/R_0A$ ) as a function of perimeter to area ratio ( $P/A$ ) for different etching recipes.  $\text{Cl}_2/\text{BCl}_3/\text{CH}_4/\text{Ar}/\text{H}_2$  recipe shows the lowest  $1/R_0A$  for all the device sizes. The nonlinear dependence of  $1/R_0A$  on  $P/A$  is an indication of surface leakage currents being dominant as compared to the bulk leakage.<sup>20</sup> For comparison,  $1/R_0A$ , assuming diffusion and generation-recombination (g-r) as the only contributing factors is plotted in Fig. 3. This curve is linear and independent of the area of the diodes. Even for the largest area diode, theoretically calculated  $1/R_0A$  is lower than the experimentally obtained values, which indicates presence of surface leakage, tunneling, and other defect related leakage currents. The contribution from the surface leakage currents becomes significant for smaller area diodes. Thus, lower values of  $1/R_0A$  for  $\text{Cl}_2/\text{BCl}_3/\text{CH}_4/\text{Ar}/\text{H}_2$  recipe indicate that the surface leakage currents in these diodes are lower as compared to the other two recipes. This is believed to be due to the formation of polymeric film on the sidewalls during etching.<sup>14,15</sup> The difference in the  $1/R_0A$  is pronounced for the smaller sized devices (higher  $P/A$ ), which have higher contribution from the surface leakage currents than bulk leakage currents. Thus, especially for the fabrication of smaller sized devices,  $\text{Cl}_2/\text{BCl}_3/\text{CH}_4/\text{Ar}/\text{H}_2$  recipe is better as compared to  $\text{Cl}_2/\text{Ar}$  and wet etching. The highest value of  $R_0A$  was obtained for 1 mm diam diode etched using  $\text{Cl}_2/\text{BCl}_3/\text{CH}_4/\text{Ar}/\text{H}_2$  and was equal to 830  $\Omega \text{ cm}^2$ . For the same sized diode,  $\text{Cl}_2/\text{Ar}$  and wet etching exhibited highest  $R_0A$  equal to 300 and 330  $\Omega \text{ cm}^2$ , respectively. This conclusively shows that  $\text{Cl}_2/\text{BCl}_3/\text{CH}_4/\text{Ar}/\text{H}_2$  etching recipe has resulted into significantly less leaky diodes as compared to  $\text{Cl}_2/\text{Ar}$  and wet etching.

**Responsivity measurements.**—The responsivity of the diodes was measured using the substitution method. In this method, the spectral response of a calibrated reference detector is transferred to the test detector by comparing the output of both devices with respect to a constant radiation source.<sup>21</sup> A  $3 \times 3 \text{ mm}^2$  PbS calibrated detector

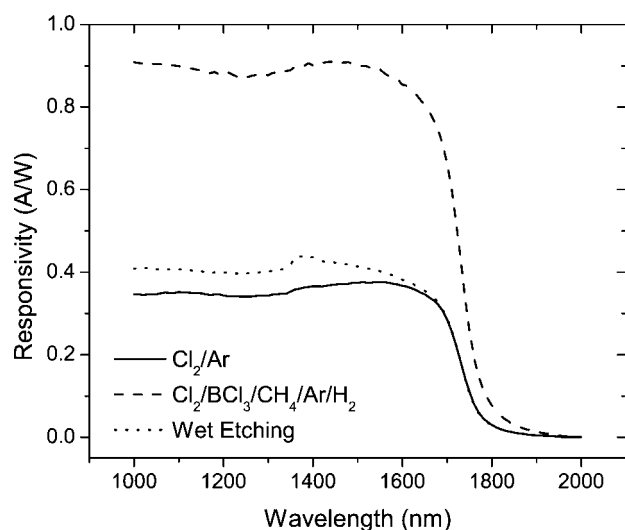


Figure 4. Responsivity of the photodiodes under zero-bias conditions.

was used as the reference. Spectral resolution of 40 nm with 0.5 and 1.5 s settling and integration times, respectively were obtained using a scan setup.<sup>22</sup>

Figure 4 shows the results of the responsivity measurements. The responsivity is constant from 1000 to 1600 nm and  $\text{Cl}_2/\text{BCl}_3/\text{CH}_4/\text{Ar}/\text{H}_2$  etched diodes show three times higher responsivity ( $\sim 0.9$  A/W) than the  $\text{Cl}_2/\text{Ar}$  and wet etched diodes ( $\sim 0.3$ – $0.4$  A/W). We propose that in unpassivated diodes, the sidewall defects act as trap centers for the photogenerated charge carriers and hence the responsivity is low. In  $\text{Cl}_2/\text{BCl}_3/\text{CH}_4/\text{Ar}/\text{H}_2$  etched diodes, these defects are considerably reduced due to passivation, which results into higher responsivity. This indicates that  $\text{Cl}_2/\text{BCl}_3/\text{CH}_4/\text{Ar}/\text{H}_2$  etching provides passivation to the diode sidewalls resulting into better electrical as well as optical properties.

### Conclusion

Summarizing, we have fabricated pn junction GaSb photodiodes using ECR plasma etching with a mixed gas recipe ( $\text{Cl}_2/\text{BCl}_3/\text{CH}_4/\text{Ar}/\text{H}_2$ ),  $\text{Cl}_2/\text{Ar}$  recipe and wet chemical etching. The diodes etched using  $\text{Cl}_2/\text{BCl}_3/\text{CH}_4/\text{Ar}/\text{H}_2$  show an order of magnitude lower leakage current density, improved ideality factor and the highest value of zero bias resistance-area product as compared to  $\text{Cl}_2/\text{Ar}$  and wet chemical etching. The spectral responsivity of the  $\text{Cl}_2/\text{BCl}_3/\text{CH}_4/\text{Ar}/\text{H}_2$  etched diodes is almost three times higher than that of the  $\text{Cl}_2/\text{Ar}$  and wet etched diodes. We speculate that the enhanced performance of these diodes is due to the incorporation of the polymer forming gas  $\text{CH}_4$  in the etching recipe, which passivated the diode sidewalls during etching. The difference

in the values of  $1/R_0A$  for the three different etching recipes becomes pronounced as we go to the smaller sized devices with  $\text{Cl}_2/\text{BCl}_3/\text{CH}_4/\text{Ar}/\text{H}_2$  recipe showing the lowest values. Further optimization of gas ratios, plasma power during etching, and temperature for the  $\text{Cl}_2/\text{BCl}_3/\text{CH}_4/\text{Ar}/\text{H}_2$  recipe should lead to improved device performance. However, even with an unoptimized recipe, better electrical and optical properties were demonstrated for the  $\text{Cl}_2/\text{BCl}_3/\text{CH}_4/\text{Ar}/\text{H}_2$  recipe when compared to the other etching methods.

### Acknowledgments

The authors thank NASA for the financial support under grant no. NAG-1-02089. In addition, this research was supported through the Missile Defense Agency and the Naval Research Laboratory under contract N00173-02-C-2046. This work was performed in part at the Cornell Nano-Scale Science & Technology Facility (a member of the National Nanofabrication Users Network) which is supported by the National Science Foundation under grant ECS-9731293, its users, Cornell University and Industrial Affiliates.

The authors assisted in meeting the publication costs of this article.

### References

1. P. S. Dutta, H. L. Bhat, and V. Kumar, *J. Appl. Phys.*, **81**, 5821 (1997).
2. M. Chyi and C. Chen, *J. Appl. Phys.*, **71**, 1237 (1992).
3. O. Hildebrand, W. Kuebart, K. W. Benz, and M. H. Pilkuhn, *IEEE J. Quantum Electron.*, **QE-17**, 284 (1981).
4. C. Hitchcock, R. Gutmann, J. Borrego, I. Bhat, and G. Charache, *IEEE Trans. Electron Devices*, **43**, 2154 (1999).
5. C. Wang, H. Choi, S. Ransom, G. Charache, L. Danielson, and D. DePoy, *Appl. Phys. Lett.*, **75**, 1305 (1999).
6. A. N. Baranov, N. Bertru, Y. Cuminal, G. Boissier, C. Alibert, and A. Joullie, *Appl. Phys. Lett.*, **71**, 735 (1997).
7. C. Mermelstein, S. Simanowski, M. Mayer, R. Kiefer, J. Schmitz, M. Walther, and J. Wagner, *Appl. Phys. Lett.*, **77**, 1581 (2000).
8. T. Maeda, J. W. Lee, R. J. Shul, J. Han, J. Hong, E. S. Lambers, S. J. Pearton, C. R. Abernathy, and W. S. Hobson, *Appl. Surf. Sci.*, **143**, 174 (1999).
9. S. J. Pearton, A. Katz, A. Feingold, F. Ren, T. R. Fullowan, J. R. Lothian, and C. R. Abernathy, *Mater. Sci. Eng., B*, **15**, 82 (1992).
10. S. J. Pearton and C. R. Abernathy, *J. Electrochem. Soc.*, **141**, 2250 (1994).
11. S. J. Pearton, F. Ren, and C. R. Abernathy, *Appl. Phys. Lett.*, **64**, 1673 (1994).
12. A. Semu and P. Silverberg, *Semicond. Sci. Technol.*, **6**, 287 (1991).
13. S. J. Pearton, U. K. Chakrabarti, A. P. Perley, and W. S. Hobson, *J. Electrochem. Soc.*, **138**, 1432 (1991).
14. C. Constantine, C. Barratt, S. J. Pearton, F. Ren, and J. R. Lothian, *Appl. Phys. Lett.*, **61**, 2899 (1992).
15. T. R. Hayes, M. A. Dreisbach, P. M. Thomas, W. C. Dautremont-Smith, and L. A. Heimbrook, *J. Vac. Sci. Technol. B*, **7**, 1130 (1989).
16. J. Sendra, J. Anguita, J. Perez-Camacho, and F. Briones, *Appl. Phys. Lett.*, **67**, 3289 (1995).
17. J. P. Langer and P. S. Dutta, *J. Vac. Sci. Technol. B*, **21**, 1511 (2003).
18. S. J. Pearton, U. K. Chakrabarti, W. S. Hobson, and A. P. Kinsella, *J. Vac. Sci. Technol. B*, **8**, 607 (1990).
19. S. R. Nukala, M.S. Thesis, Rensselaer Polytechnic Institute, Troy, NY (2000).
20. R. Ashokan, N. K. Dhar, B. Yang, A. Akhiyat, T. S. Lee, S. Rujirwat, S. Yousuf, and S. Sivananthan, *J. Electron. Mater.*, **29**, 636 (2000).
21. T. C. Larason, S. S. Bruce, and A. C. Parr, *NIST Spec. Publ.*, **1998** (Feb).
22. T. Refaat, N. Abedin, G. Koch, and U. Singh, NASA Technical Publication, NASA/TP-2003-212140, 2003.